

OXIDES OF NITROGEN SPECIES MEASUREMENTS AND ANALYSIS IN THE CENTRAL PIEDMONT OF NORTH CAROLINA, U.S.A.

DEUG-SOO KIM¹ and VINEY P. ANEJA²

¹Department of Environmental Engineering
Kunsan National University, Kunsan, Chonbuk 573-360, Korea

²Department of Marine, Earth and Atmospheric Sciences
North Carolina State University, Raleigh, N.C. 27695-8208, U.S.A.

(Received 26 August 1994)

Abstract

The quantitative knowledge of NO_y ($=\text{NO}_x + \text{HNO}_3 + \text{PAN} + \text{NO}_3 + \text{N}_2\text{O}_5 + \text{HNO}_2 + \text{NO}_3^- + \text{organic nitrates} + \dots$) distribution is essential in tropospheric chemistry, especially that related to understanding the processes leading to ozone production. Ambient concentrations of NO , NO_2 , HNO_3 and PAN as well as total NO_y were measured during June and early July 1992 at a rural site (Candor, NC), in the central Piedmont region of NC. The measurements of NO_y species were made in an effort to provide a comprehensive understanding of nitrogen chemistry and to investigate the total nitrogen budget at the site. NO_y , NO_2 and NO showed diurnal variations with maxima in the morning. The maximum NO_y concentration reached was 14.5 ppbv, and the maximum concentrations of NO and NO_2 were 5.4 and 7.8 ppbv, respectively. The mean NO_y concentration as found to be 2.88 ± 1.58 ppbv ($n=743$). The mean concentrations of NO and NO_2 were found to be 0.15 ± 0.29 ppbv ($n=785$) and 1.31 ± 0.99 ppbv ($n=769$). Products of photochemical oxidants, (NO_y - NO_x), such as HNO_3 and PAN , as well as ozone showed diurnal variation with maxima in the afternoon and minima at night. The fractions of individual reactive nitrogen species to total NO_y were investigated and contrasted to the results from remote marine site and rural continental sites. NO_x was the major species to total NO_y (45%). NO concentrations appeared to be nearly constant whether the prevailing winds were from continental areas or from oceanic areas. Linear regression of O_3 with $(\text{NO}_y - \text{NO}_x)/\text{NO}_y$ (i.e. percent NO_x converted to the photochemical products of NO_y) yielded $[\text{O}_3] = 25.8 [(\text{NO}_y - \text{NO}_x)/[\text{NO}_y] + 27]$, ($r^2=0.58$). The regression intercept is interpreted as the ozone background (intercept=27 ppbv) and the slope suggests that 8.6 molecules of ozone are formed per molecule of NO_x oxidized products (when the average NO_y concentration, about 3 ppbv at the site, is used). The NO_x/NO_y ratio was used as an indicator of the chemical age of airmasses and the ratio showed strong positive correlations with HNO_3 ($r^2=0.58$), PAN ($r^2=0.46$) and O_3 ($r^2=0.62$). Larger NO_y and NO_x/NO_y ratio were found when winds came from continental sides. It may suggest that synoptic meteorological conditions and transport of NO_x are important in the distribution of NO_y and its relationship with photochemical oxidants at the site.

1. INTRODUCTION

Recent experiments and model calculations (Wil-

liams and Fehsenfeld, 1991; Ridley and Robinson, 1992) indicate that oxides of nitrogen, NO_x ($=\text{NO} + \text{NO}_2$), play an important role in the tropospheric

chemistry. They participate not only in the acidification of precipitation but also in the formation of tropospheric ozone. Mainly NO_x reacts with ozone (O_3) and radicals, e.g. hydroxyl radical (OH) and hydroperoxyl radical (HO_2) in the atmosphere. Throughout these reactions, the concentration of NO_x plays an important role in the distribution of O_3 and the radical balance in the atmosphere. Peroxy radicals are responsible for much of the oxidation of NO to NO_2 . In the lower troposphere, ozone is formed as a by-product of the photooxidation of hydrocarbons while NO_x acts as a catalyst. Thus, the characterization of the levels of NO_x is essential to the understanding of tropospheric photochemistry. The primary pollutant, NO , is ultimately oxidized to nitric acid (HNO_3) and removed from the atmosphere by mostly heterogeneous removal processes.

NO_x lifetime in the troposphere ranges from less than a day in summer at mid-latitudes to several days in the absence of active photochemistry (Logan, 1983; Liu et al., 1987). NO_x is converted into other organic and inorganic nitrogen species such as nitric acid (HNO_3), peroxyacetyl nitrate (PAN), other organic nitrates, nitrate radical (NO_3), and particulate nitrate (NO_3^-) via photochemistry in the atmosphere. These odd-nitrogen species have relatively longer lifetimes than NO_x and some may eventually regenerate NO_x in the troposphere by thermal decomposition or photolytic reaction. Inter-conversion of NO_x into other odd-nitrogen species, therefore, can be an effective mechanism for the long range transport of reactive oxidized nitrogen to remote regions (Crutzen, 1979; Singh and Hanst, 1981).

Most of the tropospheric nitrogen species are assumed to be present as NO , NO_2 , HNO_3 , PAN, and NO_3^- (Atlas et al., 1992; Ridley, 1991; Fahey et al., 1986). Measurements of these species in rural and remote environments have, however, indicated the presence of an odd-nitrogen deficit. That is, the sum of the concentrations of the individually measured species do not add up to the concentration of NO_y ($=\text{NO}_x + \text{HNO}_3 + \text{PAN} + \text{HNO}_2 + \text{NO}_3^- + \text{organic nitrates}$) measured by total NO_y instruments. It has been suggested that unidentified odd-nitrogen species, organic nitrates, for instance, may

be present in significant enough quantities to account for the odd-nitrogen deficit. For example, Fahey et al. (1986) measured individual NO_y species and total reactive nitrogen, NO_y , at a high elevation remote site. The sum of the five individual species (NO , NO_2 , HNO_3 , PAN, NO_3^-) accounted for only 55% of the total NO_y during the summer months. The odd-nitrogen shortfall also showed seasonal variations displaying a minimum during the fall months and a maximum during the summer months. NO_y measurements during the Mauna Loa Observatory Photochemistry Experiment showed the mass contribution of the individual NO_y species measured accounted for ~75% of the total NO_y (Atlas et al., 1992), and contribution of the individual species to total NO_y at other rural/remote sites have ranged from 58% to 93% (Fahey et al., 1986; Hübler et al., 1987; Ridley et al., 1990; Buhr et al., 1990; Hübler et al., 1992).

In this paper, the partitioning of the major nitrogen species to total NO_y and the balance between the primary nitrogen species, NO_x , and total reactive nitrogen were investigated at a rural site near Candor, NC which is located in the central Piedmont of North Carolina. These observational results are important because the regional distribution of NO_y within the rural South is almost completely unknown (SOS Report, 1990). The temporal variation in the composition of NO_y is also examined and compared to that reported for other measurement sites. Additionally, an observational based analysis is performed to explore the relationship between the composition of NO_y with both photochemistry and meteorology. Because the site is indicative of a typical rural setting throughout much of the Southeast United States (being collocated to a National Dry Deposition Network (NDDN) site designated as rural), it is hoped that the analysis and discussion of the NO_y measurements made at the site may shed light on the regional characteristics of reactive nitrogen species in the Southeast United States.

2. EXPERIMENTAL

Air Quality group of North Carolina State University operates an enhanced chemistry site in the

central Piedmont region of North Carolina (35.26° N, 79.84° W, ~ 170 m MSL). Number of species, i. e. NO, total NO_x, SO₂, CO, O₃, particulates, and meteorological data are measured year round. From June 6, 1992 to July 7, 1992 an intensive measurement period was operated where NO_x, PAN, H₂O₂, HNO₃, and speciated non-methane hydrocarbons (NMHCs) were also monitored. Figure 1 shows a map of the site area and the surrounding region. The sampling site is in an open field (area ~ 1200 m²) which was previously used to grow soybeans (~ 10 years ago) and is surrounded by mixed deciduous and coniferous forest. The site is located on the eastern border of the Uwharrie National Forest. Four large urban areas of North Carolina are within a 160 km radius of the sampling site. These sources of anthropogenic pollution, Raleigh-Durham, Greensboro, and Winston-Salem as well and the junction between two busy interstate highways, I-40 and I-85, are situated to the north and northeast of the site (Figure 1) and were upwind approximately 35% of the sampling period. Charlotte is nearly due west of the site and is relatively close but was upwind only approximately 10% of the sampling period. When the prevailing wind direction is from the west, north, or northeast the site can be impacted by the more polluted air masses emanating from or crossing over these urban areas.

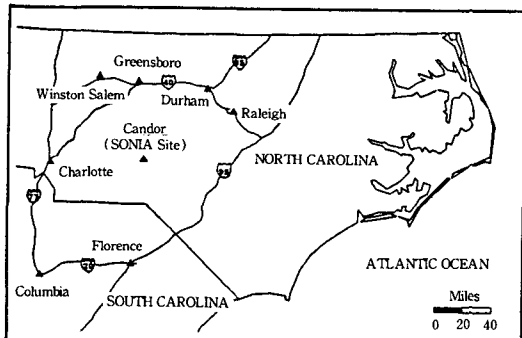


Fig 1. Map of sampling site near Candor, North Carolina.

3. METHODS

Sampling Tower

To limit sample residence time, ambient air was

drawn from a height of 10 m through a 0.76 cm I.D. glass sampling tower by an 31150 lpm blower. The residence time to the base of the tower was calculated to be ~ 0.25 seconds. A 16 port glass manifold was installed at the base of the glass sampling tower above the blower to permit sampling access. All species, with the exception of total NO_x, HNO₃, and particulate NO₃⁻, were sampled from the manifold via 5 m lengths of 0.64 cm O.D. Teflon tubing. To maximize the efficiency of NO_x conversion for the total NO_x measurement a heated molybdenum converter was mounted at the top of the 10 m tower. The NO_x sample, now converted to NO and less susceptible to loss in the sampling line, was transferred to the high sensitivity NO monitor by a 10 m long, 0.65 cm O.D. Teflon tube.

NO and NO_x

Ambient NO and NO_x were measured with a single instrument, the TECO 42S (Thermo Environmental Instruments Inc.) chemiluminescent high sensitivity analyzer. The analyzer has an internal, gold coated, heated ($\sim 325^{\circ}$ C) molybdenum converter which will convert most NO_x species to NO. For this experiment, a second heated molybdenum converter was mounted at the top of the 10 m tower and all calibrations were made using both converters. Conversion efficiency tests were conducted using certified master gas of 0.116 ppm NO₂ in N₂ (Scott Specialty Gases). The measured conversion efficiency during these tests ranged from 85 to 95%. For the laboratory operating conditions the instrument detection limit is 50 pptv for both NO and NO_x (Thermo Environmental Instruments, Inc., 1992). Six times multipoints calibrations were completed using TECO 146 multi-gas calibrator during measurement period. NO and NO_x calibration sources were certified master gases of 0.109 ppm of NO and 0.114 ppm of NO_x, respectively (Scott Specialty Gases). During the measurement period, system and performance audits were performed twice; one was an external audit performed by North Carolina Department of Environmental Health and Natural Resources (NC DEHNR) and the other was an internal audit performed by the Fleming Group in New York. Data accuracy determined from multipoints calibrations line for NO and NO₂ was 10% and 20%, res-

pectively.

HNO₃ and NO₃⁻

HNO₃ and particulate nitrate (NO₃⁻) were measured using the filter pack method (Golden et al., 1983; Parrish, 1986, 1992) in which nitrate particulates and nitric acid are sequentially collected from air drawn through a series of two filters. The first filter (1 μm Zeflur Teflon, Gelman Sciences) collects aerosols, while the second filter (1 μm Nylon, Gelman Sciences) collects HNO₃ gas. Sampling air flow rate was maintained at 24 lpm and was checked each time new filters were installed in the filter pack. The collected filters were later desorbed into a buffer solution and the solution was analyzed with an ion chromatograph to determine the nitrate content. The detection limits for both HNO₃ and NO₃⁻ are ~30 pptv.

NO₂

Ambient NO₂ was measured directly with the Scintrex LMA-3 Luminol based NO₂ analyzer. Calibrations were conducted at every week during the study period using certified master gas of 0.116 ppm NO₂ in N₂ (Scott Specialty Gases) and calibrated mass flow controller, and daily zero-span checks were employed. Ozone scrubber which was supplied by Scintrex has been installed to remove ozone interference. The scrubber is tested to remove 99.5% of O₃ at 50 ppbv. There was about 20% PAN interference in LMA-3. The uncertainty of NO₂ measurement when we assure 20% PAN interference (average PAN concentration ~0.4 ppbv) was less than 10% of NO₂ measured. We were not able to perform a field intercomparison on the LMA-3.

PAN

PAN was monitored with a custom made packed-column gas chromatograph which employed a Valco Instruments Electron Capture Detector Model 140-BN to detect the PAN peak. The GC column was a 60 cm long by 0.32 cm O.D. nickel tubing packed with 10% Carbowax 600 supported by 60/80 mesh acid-washed substrate. Retention time for the PAN peak was 2 minutes and 40 seconds or 45% of the retention time of the water vapor peak. The GC used a UHP P-5 mix (5% Methane/95% Argon) as a carrier gas. A 5 cc volume of ambient air was injected onto the column every 15 minutes

giving four data points per hour.

Calibration of the PAN GC was carried out prior to and after the field season. High concentration PAN (~15 ppmv) was synthesized by irradiating a Tedlar bag containing acetaldehyde, chlorine, and nitric oxide with ultraviolet radiation (Gay et al., 1976), and quantified by infrared spectrophotometry (Stephens, 1969). The standard preparation and quantification was performed at the EPA Environmental Research Laboratory. A multipoint calibration was then performed on the GC system by syringe injection of aliquots of the high concentration PAN mixture into bags containing metered volumes of zero grade air.

CO and SO₂

SO₂ was measured with a TECO 43S high sensitivity analyzer. The detection limit for the 43S is ~100 pptv. A TECO 48 was used to monitor CO and its detection limit is 100 ppbv. All of the instruments were calibrated according to Southern Oxidants Study QA/QC protocol.

4. RESULTS AND DISCUSSION

Figure 2 illustrates the composite diurnal profiles of nitrogen species and O₃ for the entire measurement period. Total NO_x and NO₂ show consistent maxima in the early morning hours between 06:00 and 09:00 EST with the average time of morning maximum being 07:00 EST. The mechanism most likely to be responsible for the morning peaks of the pollutants is regional transport of polluted air masses which often reached the site overnight. At sunrise, when increased solar insolation triggers the breakup of the low nocturnal boundary layer

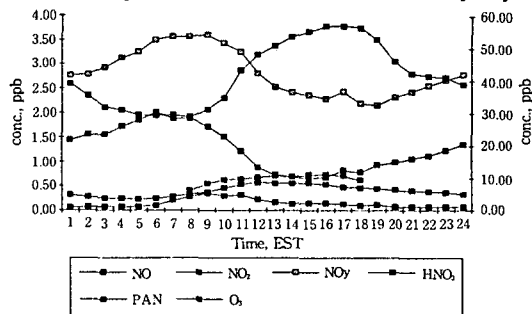


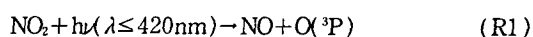
Fig. 2. Composite diurnal profiles of nitrogen species and ozone

(NBL) a period of downward mixing bring the relatively undepleted polluted air mass aloft to the surface.

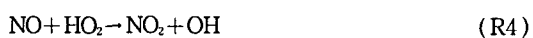
The diurnal profile of NO₂ reached a minimum during the early afternoon when solar insolation was at its peak. Daytime NO₂ is thought to be depleted mainly for HNO₃ formation; PAN and other higher order nitrates (R6 and R7 in Table 1). Increase of daytime mixing height also causes a decrease in NO₂ concentration. The NO₂ mixing ratio then gradually increases throughout the night until the rapid early morning rise to the daily maximum. This slow nighttime buildup occurs regularly in our data set and is not typically accompanied by an increase of SO₂ or CO and is thus not thought to be related to transport. An alternative hypothesis for the nighttime buildup of NO₂ is that the increase is due to natural emissions of nitrogen species from the local soils is investigated. A dynamic chamber experiment to measure nitrogen flux from soil was conducted on several different days during the measurement period (Kim et al., 1994). The results

Table 1. Chemical reactions of major reactive nitrogen species in the atmosphere.

Photostationary state (NO, NO₂ and O₃)



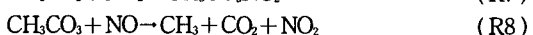
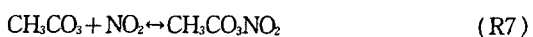
Peroxy radical disruption of photostationary state:



Formation of HNO₃



Formation and thermal decomposition of PAN, and loss of PAN with NO



of the experiment, however, show that while there was no appreciable nighttime flux of NO₂ from soil

which could explain the buildup of NO₂ at night; that frequently there was a significant level of NO flux from soil at night, typically about 2.4 ngN m⁻² s⁻¹ of NO flux. No evidence of a buildup of NO during the night was found in the data set, however. It seems, then, that a chemical mechanism may be converting the NO emitted from soil during night into NO₂, i.e. oxidation of NO by ozone. Levels of O₃ overnight are typically near 30 ppbv and are sufficient to immediately titrate any NO from the soil to NO₂ (R3 in Table 1). Rough calculation of a rate of increases in NO₂ from the soil emission using a typical NO emission rate of site was about 0.1 ppbv/hr when the height of NBL was assumed 100m. The rate of increase in NO₂ is quite consistent to the observed increase rate of NO₂ during nighttime period. This would suggest that the soil emission and the persistence of O₃ overnight at the site may facilitate the conversion of NO to NO₂ and effectively increase the background concentration of NO₂ at the site.

In Figure 2, NO shows a morning maximum between 07:00 and 09:00 EST. The time of the NO peak is sometimes the same as the NO_x, NO₂ and SO₂ peak but typically follows the NO₂ peak by one to two hours. For this reason, the existence of a morning maximum of NO mixing ratio is considered to be the combination of three different mechanisms. The first is the same mechanism that brings NO₂ to the site; medium range transport from one of the regional urban areas followed by downward mixing during the breakup of the nocturnal boundary layer. A second possible mechanism is the regeneration of NO from NO₂ after the onset of NO₂ photolysis in the morning. To test this second hypothesized mechanism, the regeneration of NO from NO₂, a simple calculation based on photostationary state equilibrium (PSS) between NO₂, O₃, and NO was made. After assuming that PSS applies early in the morning, the average 08:00 EST concentration of O₃ (~30 ppbv) and NO₂ (~2 ppbv) as well as the rate constant of the reaction of NO with O₃, $k (=1.8 \times 10^{-14} \text{ cm}^3 \text{ molecule}^{-1} \text{ s}^{-1})$, and $J (=4 \times 10^{-3} \text{ s}^{-1})$, the photolysis rate of NO₂ are used to calculate the expected concentration of NO. The resulting mixing ratio of NO is ~0.5 ppbv, a mixing ratio that is very comparable to

that observed in the morning NO profile (Figure 2). A third possible contributing factor to the morning NO peak is found in the data from the flux experiment (Kim et al., 1994). A morning increase in NO flux rates is found approximately 30% of the time in the experiment results. This natural injection of NO into the site environment could be responsible for a portion of the morning NO peak. Thus the diurnal behavior of NO is thought to be a combination of direct transport of NO_x from regional pollution sources, the regeneration of NO by the early morning near-PSS conditions, and possibly natural emission of NO from the soil.

Gaseous HNO₃ mixing ratios were measured during the daytime between 08:00 and 18:00 EST. HNO₃ shows a typical diurnal profile with a steady increase in concentration from its morning minimum to a maximum occurring at ~15:00 EST followed by a steady decrease to nighttime lows. The diurnal profile of HNO₃ is explained by the mechanism of the daytime formation of nitric acid. HNO₃ is primarily produced through the reaction of NO₂ with OH during the daytime (R6 in Table 1). In fact, HNO₃ typically starts to increase at the same time NO₂ mixing ratios begin to decline and the HNO₃ maximum corresponds with the NO₂ minimum in the middle afternoon (Figure 2). Statistically, there was found to be a negative correlation ($[HNO_3] = -0.14[NO_2] + 0.86$, $r^2=0.4$) between diurnal profiles of NO₂ and HNO₃ in our data.

PAN exhibits a typical diurnal profile very similar in shape and magnitude to profiles observed by Singh and Salas (1989) for northeastern U. S. cities. The minimum concentration occurs between 03:00 and 06:00 EST and a broad maximum is found between 12:00 and 15:00 EST shortly after the solar radiation maximum. The relationship between PAN and solar radiation maxima suggests that local photochemical production of PAN may be important at the site. Additionally, since the thermal lifetime of PAN is relatively short (~2.3 hrs) during a warmer temperatures (25°C with an NO/NO₂ ratio of 0.3) such as those typical of the North Carolina summer, the effectiveness of even medium range transport of PAN is not likely to be great (Shepson, et al., 1992). It is entirely possible, however, that medium range transport is

responsible for the presence of PAN precursors at the site.

The nighttime minimum of PAN is attributed to the presence of a nocturnal boundary layer which is characterized by statically stable air with weaker, sporadic turbulence and is isolated to the lowest 100 to 200 m of the troposphere. Increased surface deposition as well as thermal decomposition (R7 in Table 1) followed by reaction of the peroxyacetyl radical with NO (R8 in Table 1), perhaps that emitted from the local soil, leads to the rapid loss of PAN in the night. PAN concentrations never dropped below the detection limit of the instrument (50 pptv), however, and often remain as high as 300 pptv throughout the night.

Relationships Between NO_x and Its Constituent Species

Table 2 presents statistical summaries of the average, daytime, and nighttime concentrations of individual odd-nitrogen compounds and total NO_x measured at the site. Daytime is defined as 07:00-17:00 EST and nighttime as 20:00-04:00 EST. All concentrations reported in this table are based on hourly averages integrated over the measurement period except for nitric acid which is a two

Table 2. Statistical summaries of the average, daytime and nighttime concentrations of individual nitrogen species and total NO_x measured at Candor site.

Species	data set	n	Max.	Mean	Med.	St.Dev.
NO	day	357	1.46	0.22	0.14	0.23
	night	299	5.41	0.09	0.04	0.33
	all	785	5.41	0.15	0.07	0.29
NO ₂	day	336	5.06	1.19	0.91	0.96
	night	302	7.84	1.38	1.25	0.91
	all	769	7.84	1.31	1.06	0.99
PAN	day	267	1.17	0.48	0.46	0.27
	night	216	0.86	0.33	0.32	0.17
	all	578	1.17	0.40	0.36	0.24
HNO ₃	day	250	1.76	0.67	0.66	0.33
NO _x	day	333	9.31	2.97	2.78	1.49
	night	291	14.47	2.77	2.68	1.59
	all	743	14.47	2.88	2.70	1.58
ΣNO _x	day	148	5.55	2.38	2.25	1.04

hour average and was measured only during daytime. The partitioning of NO_x among individual odd-nitrogen compounds for all data are given in Table 3. The fractional contribution of each odd-ni-

trogen compound measured recently at several different sites in the U.S. are also presented in Table 3.

Table 3. Partitioning of NO_x among individual nitrogen species at Candor site and recent results from other rural sites in the U.S.

Species	n	Max.	Mean	Med.	St. Dev.	Scotia	Niwot Ridge	Mauna Loa
NO/NO_x	568	0.38	0.05	0.03	0.05	—	—	—
NO_2/NO_x	577	1.02	0.41	0.38	0.22	—	—	—
NO_x/NO_y	568	1.40	0.45	0.41	0.27	0.59	0.32	0.14
PAN/NO_x	488	0.64	0.13	0.12	0.08	0.14	0.24	0.05
HNO_3/NO_x	180	0.64	0.21	0.19	0.11	0.16	0.13	0.43
$\Sigma\text{NO}_y/\text{NO}_x$	180	—	0.80	0.72	—	0.93	0.73	0.75

Generally, concentrations of individual compounds during daytime are higher than those in nighttime except for the NO_2 concentration. Lower concentrations in nighttime can be attributed to the presence of stable NBL which isolates the lowest ~100 m of the atmosphere from daytime mixed layer thus allowing the depletion of the species through surface deposition. The reason for the exception of NO_2 is a combination of the times chosen as the definition for day and night, photochemical depletion of NO_2 during the day, and the buildup of NO_2 overnight as described above. The bulk of the transported NO_2 arrived typically between 06:00 and 08:00 EST and is often not included in the calculation of either the daytime or nighttime average mixing ratio. Therefore, the day and night concentrations are not influenced by the spikes of high NO_2 brought to the site by transported air masses. As pointed out above, NO_2 is typically depleted during the middle of the day by its photolysis reaction (R1 in Table 1) and/or terminating reaction with OH (R6 in Table 1), and is at a relatively low mixing ratio. Additionally, NO_2 often builds up over night and there are a number of instances of early morning, i.e. 03:00–04:00 EST, transport episodes at the site.

Comparison of the fractions of HNO_3 and NO_x for the remote marine site and continental sites in Table 3 shows that the fraction contribution of HNO_3 to NO_x (0.43) is significantly higher than the contribution of NO_x to NO_y (0.14) at a remote ma-

rine site, Mauna Loa. In contrast, for the rural continental sites (Niwot Ridge, Scotia and site Candor) NO_x is the primary contributor to total NO_y (NO_x/NO_y ratio ranged in 0.32–0.59.).

In Table 4 the average daytime concentrations and fractional contributions of each species to NO_x are reported by wind sector. The relatively large contribution of NO_x to NO_y from the continental wind directions again indicates that these air masses are more heavily impacted by anthropogenic pollution. For the easterly winds representing the more oceanic air masses the fractional contribution of HNO_3 is at its highest and the contribution of NO_2 is at its lowest. These results may support the theory that the easterly winds are bringing oceanic air masses to the site. It is also interesting to note that the fractional contribution of NO_2 is decreased in the easterly sector but the ratio of NO/NO_2 (0.52) is also significantly higher than that of the continental air masses (0.19) in the other sectors. In fact, with the exception of the westerly data, which suffers from a small number of data point, the NO mixing ratio appears to be nearly independent of wind direction. This independence may support the idea of a relatively important local source of NO at the site, namely emission from soil.

Table 3 and 4 also indicate the site has an odd-nitrogen deficit of ~0.20 which is comparable to that found in recent field experiments conducted at Niwot Ridge, Colorado; Scotia, Pennsylvania; and Mauna Loa, Hawaii (Fahey et al., 1986; Buhr et

al., 1990; Atlas et al., 1992). Daily deficits varied from an actual excess of odd-nitrogen compounds, that is the sum of the individual species exceeded the total NO_y measurement, to a deficit as large as 40%. There are a number of possible sources for the odd-nitrogen deficit. The first to be considered is the accuracy of the instrumentation used to monitor these species and the accuracy of available calibration techniques. Especially at the low mixing ra-

tios encountered at a rural site such as site Candor, there is a margin of error associated with each instrument used that could well explain a portion of the deficit. While every effort is taken to minimize the impact of instrument uncertainty and to calibrate the instruments as accurately as possible the likelihood of some degree of inaccuracy in the reported values must be considered.

Table 4. Average daytime concentrations and fractions of total NO_y , by wind sectors.

Species	Conc. and partitions	Northerly	Southerly	Easterly
NO	avg, ppbv	0.25	0.27	0.29
	% NO_y	7%	8%	14%
NO_2	avg, ppbv	1.33	1.41	0.56
	% NO_y	37%	42%	30%
NO_x	avg, ppbv	1.58	1.68	0.85
	% NO_y	46%	52%	41%
PAN	avg, ppbv	0.58	0.44	0.30
	% NO_y	15%	12%	13%
HNO_3	avg, ppbv	0.70	0.63	0.62
	% NO_y	22%	21%	27%
NO_y	avg, ppbv	3.46	3.23	2.09
	avg. $\Sigma \text{NO}_y / \text{NO}_y$	0.81	0.84	0.84
O_3	avg, ppbv	39	45	54
	avg. O_3 / PAN	68	101	177
PAN/ NO_x	avg.	0.38	0.26	0.35
NO / NO_2	avg.	0.19	0.19	0.52

The consistency of the deficit from experiment to experiment and from day to day in our own measurements does, however, suggest that there are some species which are either being underestimated due to measurement technique limitations or are simply not being detected at all. Contenders for undetected species are higher order peroxyacetyl nitrates (i.e., PPN, MPAN, PBZN) and alkyl nitrates (i.e., RONO_2). These compounds were not detected by the PAN GC at site Candor. PPN, in particular, is often reported as having mixing ratios that are ~10% of the mixing ratio of PAN. To ensure that there was no problem with the PAN GC that was preventing the detection of higher order organic nitrates, PPN, PnBN, PBZN, MPAN, and Methyl Nitrate were all synthesized and injected onto the GC in the laboratory following the experiment. All of the species were detected by the GC at

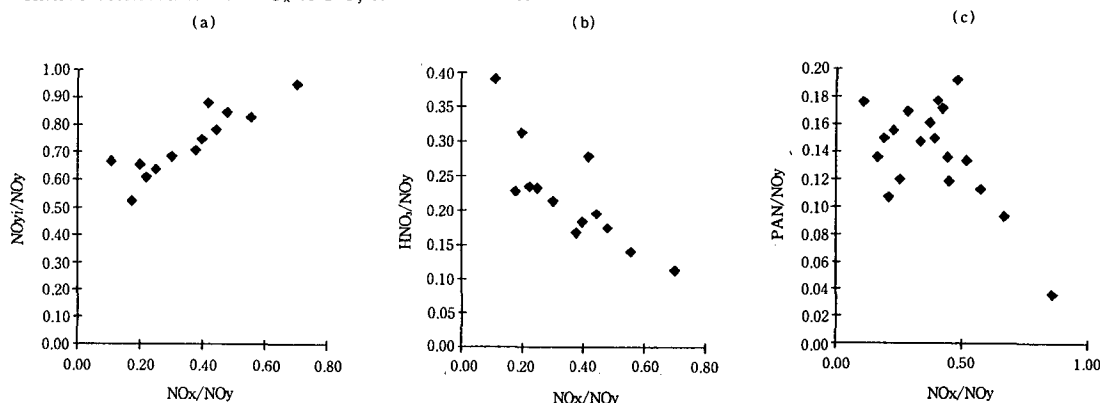
ppb level concentrations but might not have been detected in the field if they were present at low pptv levels.

There is evidence in support of the organic nitrate theory as well. In Table 4 it appears that the nitrogen deficit is greater in the northerly wind direction, the wind direction most heavily impacted by urban air masses. If higher order organic nitrates were the culprit in the nitrogen deficit this relationship with wind direction would be plausible. The greater levels of NMHCs along with higher NO_x expected from urban air masses improve the possibility of the formation of organic nitrate compounds. These compounds, particularly the higher order peroxyacetyl nitrates, are known to be less stable than PAN and have been shown to deplete more rapidly as the air mass moves away from its source and would be expected to be more prevalent

in more recently polluted air masses from the north (Singh and Salas, 1989).

Additional evidence in support of the organic nitrate theory is shown in Figure 3(a). It is a plot of the fraction of total NO_y accounted for by the sum of individual nitrogen species ($\text{NO}_{y,i}/\text{NO}_y$) plotted against the NO_x/NO_y ratio. Figure 3(a) clearly shows that the nitrogen deficit is largest when the relative contribution of NO_x to NO_y is smallest. This

trend suggests that the deficit consists of NO_y species other than NO and NO_2 . Organic nitrates certainly fall in this category. HNO_3 also falls in this category and an underestimation of HNO_3 could also be part of the nitrogen deficit. The existence of a nitrogen deficit at several sites is a vexing one and more research needs to be conducted in this area.



Figures 3 (a), 3 (b), and 3 (c). Variation of the fraction of $\sum \text{NO}_{y,i}$, HNO_3 , and PAN to total NO_y versus NO_x/NO_y . Each cell represents 20 data points and the cells are sorted in ascending order of NO_x/NO_y .

NO_x and the Ratio of NO_x/NO_y

NO_x is the most abundant portion of NO_y at Candor site during the measurement period. The average fraction of NO_x/NO_y was 0.45. In the absence of high deposition and dispersion the total quantity of NO_y can be conserved while the lifetime of NO_x is limited to as little as 1 day or less in the boundary layer (Spicer, 1977). The lifetime of NO_x depends strongly on the physical (wet and dry deposition) and chemical processes in the atmosphere. The obvious importance of photochemistry is in the rapid conversion of NO_x into longer lived reservoir species such as PAN and HNO_3 (R6, R7 in Table 1). Thus the relative abundance of NO_x in the atmosphere can be used as an index of the photochemical age of the air mass (Ridley, 1991). The ratio of NO_x/NO_y reflects the degree of transformation of NO_x species to reservoir species of NO_y , but is not skewed by dilution effects or changes in the total magnitude of the concentration of nitrogen species. The NO_x/NO_y ratio is expected to be nearly one in a freshly polluted air mass while the

ratio should decrease as the air mass ages photochemically and NO_x is converted to other NO_y species. Thus we expect a relatively high value of NO_x/NO_y in an air mass encountered a relatively short time after its exposure to anthropogenic pollution and a significantly lower value for the ratio for an air mass encountered long after its exposure to pollution. Recent measurements show that the average NO_x/NO_y ratio in the planetary boundary layer increases from 0.11 over the ocean (Mauna Loa, Atlas, 1992) to as high as 0.59 over a continental rural site (Scotia, PA, Ridley, 1991).

In Figure 3(b) and (c) the ratios of HNO_3/NO_y and PAN/NO_y are plotted against NO_x/NO_y . The ratio of PAN/NO_y and HNO_3/NO_y decreases as the ratio of NO_x/NO_y increases. The similar explanation as that for Figure 4 is used for the relationships shown in these plots. Plots of PAN and O_3 concentrations against the NO_x/NO_y ratio are shown in Figure 3(d) and (e). Again, PAN increases in concentration strongly as the NO_x/NO_y ratio decreases to an inflection point of 0.45. There

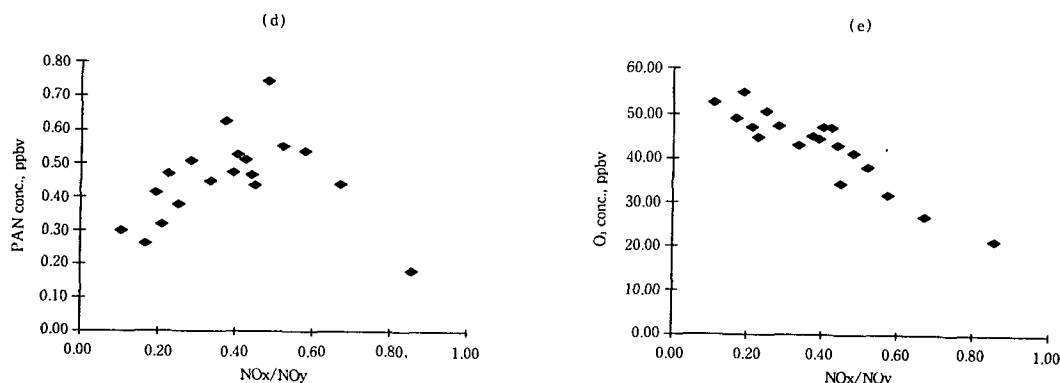


Figure 3 (d) and 3 (e). Variation of PAN and O_3 with NO_x/NO_y . Each cell represents 20 data points and the cells are ordered by ascending NO_x/NO_y .

after, PAN concentration decreases linearly with decrease of NO_x/NO_y ratio. It is believed that thermal decomposition (i.e. relatively short lifetime) in older air masses ultimately depletes peroxyacetyl radical thereby reducing the contribution of PAN to total NO_y in older air masses. In contrast, O_3 concentration increases linearly with decreasing NO_x/NO_y throughout the entire range of NO_x/NO_y . The relationship of O_3 to NO_x/NO_y is quite similar to the relationship between HNO_3/NO_x and NO_x/NO_y (Figure 3(b)). As the ratio of NO_x/NO_y decreases a portion of that decrease can be attributed to the formation of organic nitrate compounds, particularly PAN. O_3 continues to increase with decreasing NO_x/NO_y , however, while PAN at some point will begin to decrease with decreasing NO_x/NO_y , because O_3 has a significantly longer lifetime (~ 30 days) than PAN (\sim few hours). The relationship of both PAN and O_3 to NO_x/NO_y may also be explained by examination of the local photochemical and transport process. The NO_x/NO_y ratio is typically at its maximum early in the morning when NO_x is mixed downward at the breakup of the NBL. At this time PAN and O_3 concentrations are typically near their minimum. In addition, peaks of transported O_3 and PAN rarely arrive with the NO_x peaks in the morning and when transport does occur simultaneously between NO_x , PAN, and O_3 the magnitude of the transported PAN and O_3 is significantly smaller than that of NO_x . Thus it appears that PAN and O_3 form mostly as a result of photochemical reactions involving transported and perhaps locally generated precursor species.

Figure 4 shows the plots of HNO_3/NO_x vs NO_x and PAN/NO_x vs NO_x , respectively. Using the absolute level of NO_x as a gauge of chemical age, Figure 4 illustrates the photochemical transformation of the active nitrogen species into the reservoir species HNO_3 and PAN. This transformation is an illustration of the air mass aging process and of local photochemical processes. There is strong correlation between the variables in each of the plots where both the HNO_3/NO_x ratio and PAN/NO_x ratio increase strongly as NO_x decreases. This relationship is expected because NO_x decreases and is converted to reservoir NO_y species as the air mass ages during transport. Also, the average diurnal profiles of NO_x , PAN, and HNO_3 clearly show that, on a local photochemical basis, both PAN and HNO_3 reach their maxima when NO_x is near its minimum at the site. These two factors of photochemical aging of a transported air mass and the impact of local photochemistry at the site combine to explain the trends shown in Figure 4. Similar trends have been observed in the troposphere (Hubert, et al., 1990; Ridley, 1991) even though the range of the ratios and NO_x levels are different because of the different nature of the experimental environment.

As stated above, for a given air mass the NO_x/NO_y ratio provides a relative measure of the extent of photochemical interconversion between NO_x and the balance of the NO_y reservoir. The ratio therefore is expected to have a diurnal profile that corresponds with the driving force behind photochemical activity, solar radiation. To remove any bias from the magnitude of the concentrations of the nitrogen

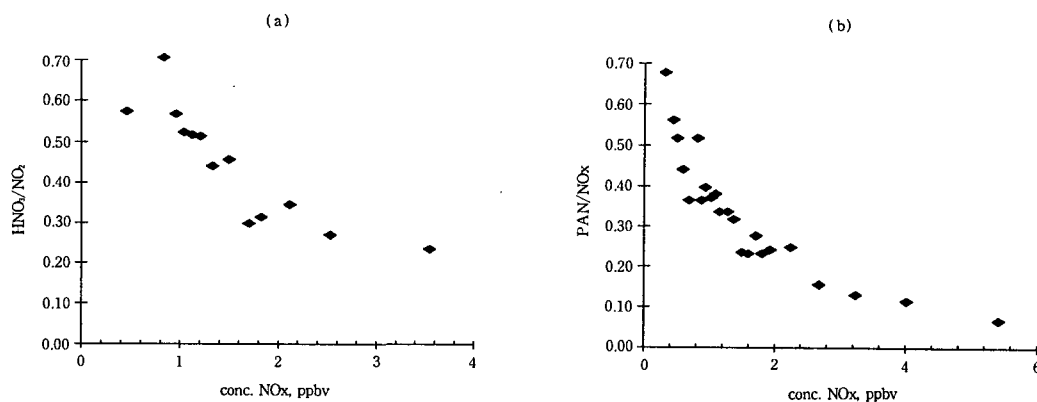


Fig 4. Ratio of HNO_3/NO_x and PAN/NO_x versus NO_x . Each cell represents 10(a) or 20(b) data points and the cells are sorted in increasing order of NO_x .

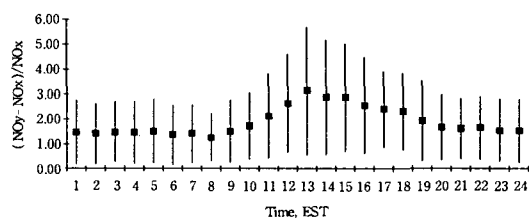


Fig 5. Composite diurnal profile of $(\text{NO}_y - \text{NO}_x)/\text{NO}_x$ for the entire measurement period

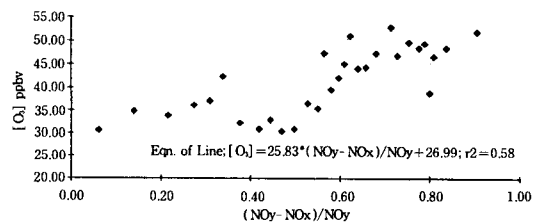


Fig 6. Variation of O_3 versus the ratio $(\text{NO}_y - \text{NO}_x)/\text{NO}_y$.

species the difference between NO_y and NO_x can be normalized by NO_x , i.e. $(\text{NO}_y - \text{NO}_x)/\text{NO}_x$. Figure 5 shows the diurnal variation in the $(\text{NO}_y - \text{NO}_x)/\text{NO}_x$ ratio at the site. The ratio reaches a maximum value at midday when local photochemical activity reaches its peak. The observed range of the ratio at the site is 1 to 4, a range that compares favorably with the results from Niwot Ridge in Colorado (Fahey, et al., 1986). The average NO_y/NO_x ratio for each hour in the diurnal cycle was typically $\sim 13\%$ higher at Candor site than at Niwot Ridge. The discrepancy is probably due to the lesser impact of anthropogenic sources on a regular basis because of the high altitude nature of the Niwot Ridge site. Niwot Ridge is frequently impacted by free tropospheric air masses which are less effected by anthropogenic sources of NO_x . Figure 6 shows a plot of O_3 against $(\text{NO}_y - \text{NO}_x)/\text{NO}_y$. This plot shows the relationship between O_3 and the degree of conversion of NO_x to reservoir species of NO_y , i.e. $(\text{NO}_y - \text{NO}_x)$. The slope of the plot indicates the amount of O_3 production for a given amount of NO_x conversion in the air mass. O_3 increases as photochemical

conversion rate of NO_x increases. A linear regression of O_3 and $(\text{NO}_y - \text{NO}_x)/\text{NO}_y$ is $[\text{O}_3] = 25.8 * ((\text{NO}_y - \text{NO}_x)/\text{NO}_y) + 27$, $r^2 = 0.58$). Applying ~ 3 ppbv of average NO_x concentration at the site, the slope of regression suggests that 8.6 molecules of O_3 are formed for every molecule of NO_x conversion to NO_y , and intercept is interpreted as 27 ppbv of ozone background. Similar statistical relationship between ozone and photochemical productions of nitrogen species have been reported, resulting from north-eastern rural continental sites measurements (Trainer et al., 1993). Ozone concentration is expected to be low in young air masses because in the troposphere O_3 is mainly formed by the same photochemical processes that lead to the conversion of NO_x into reservoir species such as PAN and HNO_3 . Thus, as the ratio increases, indicating a more aged air mass and more complete photochemical conversion of NO_x to reservoir species of NO_y , the concentration of O_3 also increases. In fact, it is expected that the ratio of O_3 to reservoir NO_y should increase as air mass age increases because of the relatively longer lifetime of O_3 than that of reservoir NO_y spe-

cies such as HNO_3 and PAN. In a very old air mass with the value of the $(\text{NO}_y - \text{NO}_x)/\text{NO}_y$ ratio approaching unity the O_3 should continue to increase while the reservoir NO_y species begin to decrease due to their shorter lifetimes.

5. CONCLUSIONS

Each species showed diurnal variations (Figure 2). NO_y , NO and NO_2 maxima occurred in the morning between 05:00 and 09:00 EST. The NO_y and NO_2 maxima typically occurred around 07:00 EST and was often accompanied by an SO_2 peak. It is likely that the NO_x and SO_2 were mixed down to the surface during the morning breakup of the NBL. The NO peak at the site could also be supplied by downward mixing of polluted air masses but the short lifetime of NO and the lack of strong correlation between the NO_2 and NO peak suggests other mechanisms may be at work. Possible other mechanisms responsible for the NO peak at 09:00 EST are conversion of NO_2 to NO by photolysis and peroxy radicals available at the time in the morning or natural NO flux from the soil. A flux experiment conducted over the measurement period showed elevated morning flux of NO in 30% of the samples. PAN, HNO_3 and O_3 diurnal variation were quite similar suggesting they might share a common source, probably mesoscale photochemical production from transported and locally produced precursor species.

NO_2 was the most abundant of NO_y species accounting for ~38% of total NO_y (Table 3). These results are significantly different than those obtained from a remote marine site but were comparable with recent results from two other rural continental sites (Niwot Ridge, Colo., and Scotia, Pa.) in the United States. The discrepancy between the NO_y partitioning at Candor site and the marine site are attributed to the influence of regional anthropogenic sources of NO_y and the continental origin of the majority of air masses encounter at the site.

The NO_x/NO_y ratio as well as the quantity $(\text{NO}_y - \text{NO}_x)/\text{NO}_y$ were used as 'chemical clocks' of an air mass and the photochemical oxidants were correlated with these measures of air mass age (Figure 3 and 6). Linear regression of O_3 on $(\text{NO}_y - \text{NO}_x)/\text{NO}_y$

yielded the $[\text{O}_3] = 25.8(\text{NO}_y - \text{NO}_x)/\text{NO}_y + 27$. Such a statistical relationship may have temporal and spacial variations due to the complexity of the formation of ozone that involves volatile organic compounds (VOC) and NO_x precursors (Trainer et al., 1993). The similarity of the relationship in regional homogeneity may permit reasoning without resulting to specifying the complex chemistry in the lower troposphere associated with the formation of ozone in that specific environment. Using 3 ppbv of average NO_y concentration at the site, slope of the regression suggests that 8.6 molecules of ozone are produced for every one molecule of NO_x conversion to oxidized species. It was comparable to the results of Trainer et al. in eastern rural continental sites. This similarity suggests that at rural sites in the eastern continental U.S. these statistical relationships may be used to approximate the complex ozone formation chemistry but without detail VOC measurements.

In conclusion, while this study has shed some light on the behavior of reactive odd-nitrogen compounds in the southeast U.S., it is clear that more comprehensive research into the role of naturally produced nitrogen species and its characteristics and the behavior of photochemical oxidants is needed to enhance our understanding of the chemical climatology of the southeast U.S.. Such knowledge will be required if an accurate chemical model to research atmospheric chemistry in this area or region is to be developed. The understanding gained from field research and future chemical models developed based on data collected in field research are of great importance to the formation of basic pollution control policy in the southeast U.S..

Acknowledgements-This research has been funded by the U.S. Environmental Protection Agency through a cooperative agreement with the University Corporation for Atmospheric Research (S 9192) as part of the Southern Oxidant Study-The Southern Regional Oxidant Network (SOS-SERON). We acknowledge Dr. W. Lonneman, U.S. EPA for assisting us in the PAN measurements; Mr. G. Murray, N.C. DENHR for systems audit; Dr. H. Jeffries, UNC at Chapel Hill, Dr. B. Gay, U. S. EPA, Dr. M. Rodgers, Ga Tech, and members of

our Air Quality group, Zheng Li, Mita Das and Eric Ringler for their assistance and discussions on atmospheric oxidants; and Ms. B. Batts in the preparation of the manuscript.

Disclaimer-The contents of this document do not necessarily reflect the views and policies of the U. S. Environmental Protection Agency, the University Corporation for Atmospheric Research, nor the views of all members of the Southern Oxidants Study Consortia, nor does mention of trade names or commercial or non-commercial products constitute endorsement or recommendation for use.

6. REFERENCES

- Atlas, E. L., Ridley B.A., Hubler G., Walega J.G., Carroll M.A., Montzka D.D., Huebert B.J., Norton R.B., Grahek F.E., and Schauffler S. (1992) Partitioning and budget of NO_x species during the Mauna Loa Observatory Photochemistry Experiment, *J. Geophys. Res.*, 97, 10449-10462.
- Buhr, M. P., Parrish D.D., Norton R.B., Fehsenfeld F.C., Sievers R.E., and Roberts J.M. (1990) Contribution of organic nitrates to the total odd nitrogen budget at a rural eastern U. S. site, *J. Geophys. Res.*, 95, 9809-9816.
- Crutzen, P. J. (1979) The role of NO and NO_2 in the chemistry of the troposphere and stratosphere, *Annu. Rev. Earth Planet Sci.*, 7, 443-472.
- Fahey, D. W., Hubler G., Parrish D.D., Williams E. J., Norton R.B., Ridley B.A., Singh H.B., Liu S.C., and Fehsenfeld F.C. (1986) Reactive nitrogen species in the troposphere: Measurements of NO , NO_2 , HNO_3 , particulate nitrate, peroxyacetyl nitrate (PAN), O_3 , and total reactive nitrogen (NO_x) at Niwot Ridge, Colorado, *J. Geophys. Res.*, 91, 9781-9793.
- Gay, B.W., Noonan, R.C., Bufalini, J.J., Hanst, P. L., Photochemical synthesis of peroxyacyl nitrates in gas phase via chlorine-aldehyde reaction. *Environ. Sci. Technol.*, 10, 82. 1976.
- Golden, P.D., Kuster W.C., Albritton D.L., Fehsenfeld F.C., Connel, P.S., Norton R.B., and Huebert B.J., (1983) Calibration and tests of the filter-collection method for measuring clean air, ambient levels of nitric acid. *Atmospheric Environment*, 17, 1355-1364.
- Hubler, G., et al. (1987) Partitioning of reactive odd nitrogen species in the tropospheric boundary layer, paper presented at the 6th International Symposium of the commission for Atmospheric Chemistry and Global Pollution, Peterborough, Ontario, Canada, August 23-29, 1987.
- Hubler, G., Fahey D., and Ridley B.A. (1992) Airborne measurements of total reactive odd nitrogen NO_x , *J. Geophys. Res.*, in press.
- Huebert B. J., et al. (1990) Measurements of the nitric acid to NO_x ratio in the troposphere, *J. Geophys. Res.*, 95, 10193-10198.
- Kim, D.S., Aneja V.P. and Robarge W.P. (1994) Characterization of nitrogen oxide fluxes from soil of a fallow field in the Central Piedmont of North Carolina. *Atmospheric Environment*, 28, 1126-1137.
- Liu, S.C., Trainer M., Fehsenfeld F.C., Parrish D. D., Williams E.J., Fahey D.W., Hubler G., and Murphy P.C. (1987) Ozone production in the rural troposphere and the implication for regional and global ozone distributions, *J. Geophys. Res.*, 92, 4191-4207.
- LMA-3 LUMINO_x Operation Manual, SCINTREX/UNISEARCH, Concord, Ontario, Canada, 1987.
- Logan, J. A. (1983) Nitrogen oxides in the troposphere; Global and regional budgets, *J. Geophys. Res.*, 88, 10785-10807.
- Parrish D.D., Norton R.B., Bollinger M.J., Liu S.C., Murphy P.C., Albritton D.L., Fehsenfeld F.C. and Huebert B.J. (1986) Measurements of HNO_3 and NO_3 -particulates at a rural site in the Colorado mountains, *J. Geophys. Res.*, 91, 5379-5393.
- Parrish D.D., Hahn C.J., Williams E.J., Norton R. B., Fehsenfeld F.C., Singh H.B., Shetter J.D., Grandrud B.W., and Ridley B.A. (1992) Indications of photochemical histories of Pacific air masses from measurements of atmospheric trace species at Point Arena, Califor-

- nia, *J. Geophys. Res.*, 97, 10285-10290.
- Ridley, B. A. and Robinson E. (1992) The Mauna Loa Observatory Photochemistry Experiment, *J. Geophys. Res.*, 97, 10285-10290.
- Ridley, B. A.(1991) Recent measurements of oxidized nitrogen compounds in the measurements, *Atmospheric Environment*, 21, 569-578.
- Ridley, B.A., Shetter J.D., Walega J.G., Madronich S., Elsworth C.M, and Grahek F. (1990) The behavior of some organic nitrates at Boulder and Niwot Ridge, Colorado, *J. Geophys. Res.*, 95, 13949-13962.
- Shepson, P. B., Hastie D.R., So K.W., Schiff H.I., and Wong P.(1992) Relationship between PAN, PPN and O₃ at urban and rural sites in Ontario, *Atmospheric Environment*, 26A, 1259-1270.
- Singh, H. B. and Hanst P.L.(1981) Peroxyacetyl nitrate (PAN) in the unpolluted atmosphere; An important reservoir for nitrogen oxides, *Geophys. Res. Lett.*, 8, 941-.
- Singh, H. B. and Salas L.J.(1989) Measurements of peroxyacetyl nitrate(PAN) and peroxypropionyl nitrate(PPN) at selected urban, rural and remote sites, *Atmospheric Environment*, 23, 231-238.
- Spicer, C. W.(1977) The fate of nitrogen oxides in the atmosphere, in *Advances in Environmental Science and Technology*, vol. 7, edited by J. N. Pitts, Jr., and R. L. Metcalf, pp. 182-197, John Wiley, New York, 1977.
- Stephens, E.R., *The Formation, Reactions, and Properties of Peroxyacyl Nitrates PANs in Photochemical Air Pollution. Advances in Environmental Sciences and Technology, I*, 119-146, 1969.
- Thermo Environmental Instruments Inc. (1992) Instruction Manual Model 42(S): Chemiluminescence NO-NO₂-NO_x analyzer, Designated reference method number RFNA-1289-074, Thermo Environmental Instruments Inc., Franklin, MA, 1992.
- Trainer M et al.(1993) Correlation of ozone with NO_x in photochemically aged air, *J. Geophys. Res.*, 98, 2917-2925.
- Williams, E. J. and Fehsenfeld F.C. (1991) Measurement of soil nitrogen oxide emissions at three north American ecosystem, *J. Geophys. Res.*, 96, 1033-1042.